

Cracked concrete structures under cyclic load

Fabrizio Barpi & Silvio Valente

Department of Structural and Geotechnical Engineering, Politecnico di Torino, Torino, Italy

ABSTRACT: The safety of cracked concrete dams is fundamentally affected by their mechanical behaviour under seismic excitation. Such a load is far from being harmonic and is characterized by intermittent spikes. Therefore the sequence effect is analysed. Two widely accepted non-linear methods were used: the *Cohesive Crack Model* to analyse the evolution of the process zone and the *Continuous Function Model* (CFM) to analyse the local hysteresis loop. In its original formulation, CFM predicts that a higher preloading arrests the fatigue crack growth at a subsequent lower load level. This unrealistic and unconservative behaviour is due to the fact that the above mentioned model neglects the damage occurring during the so-called inner-loops. In other words the CFM assumes that inner loops are mere loading loops and not fatigue loops. This assumption causes an incorrect prediction of the sequence effect. For the same reason the CFM predicts an endurance limit which is higher than attested by experimental evidence. In order to obtain more realistic results, in the present paper the CFM was enhanced, introducing a damage mechanism for the inner loops too. In the new model proposed, as well as in the original CFM, the endurance limit is seen to be almost constant relative to structural size.

Keywords: cohesive, concrete, crack, cyclic, endurance, fatigue, fracture

1 INTRODUCTION

The safety of cracked concrete dams is fundamentally affected by their mechanical behaviour under seismic excitation. It is well known that concrete presents a diffused damage zone within which micro-cracking increases and stresses decrease as the overall deformation increases. This results in the softening of the material in the so-called *fracture process zone* (FPZ), whose size can be compared with a characteristic dimension of the structure. This dimension is not constant and may vary during the evolutionary process. In this context, a numerical method has to be used together with the *cohesive* or *fictitious* crack model as shown by Hillerborg et al. The interaction between strain-softening and fatigue behaviour is analysed by modeling the hysteresis loop under unloading-reloading conditions.

2 DESCRIPTION OF THE MICROMECHANICAL MODEL FOR THE PROCESS ZONE

In each point of the fictitious process zone a micromechanical approach to tension softening is used according to a strategy proposed in Huang & Li (1989) and Karihaloo (1995). Tension softening behaviour appears when the damage in the material has localized along possible fracture planes. This behaviour has been successfully modelled using two- and three-dimensional micromechanical models.

All models provide a relationship between residual tensile stress carrying capacity and crack opening displacement (*COD*) as a function of known concrete microstructural parameters (included in factor β), e.g. aggregate volume fraction V_f , Young's modulus E_c , ultimate tensile strength f_t and fracture toughness of the

homogenized material K_{Ic}^{hom} (see Figure 1). According to these models, the function is assumed to be:

$$\frac{w}{w_c} = \underbrace{\frac{(K_{Ic}^{hom})^2}{E_c(1 - V_f)f_t}}_{\beta} \frac{f_t}{\sigma} \left[1 - \left(\frac{\sigma}{f_t} \right)^3 \right] \quad (1)$$

Figure 1 shows the unloading and reloading loop, according to the so-called *Continuous Function Model* proposed by Hordijk. This model is based on uniaxial tension test results and has been used successfully in the interpretation of four-point bending tests through the so-called multilayer beam model (Hordijk (1991)). Unloading and reloading loops are magnified in Figure 2.

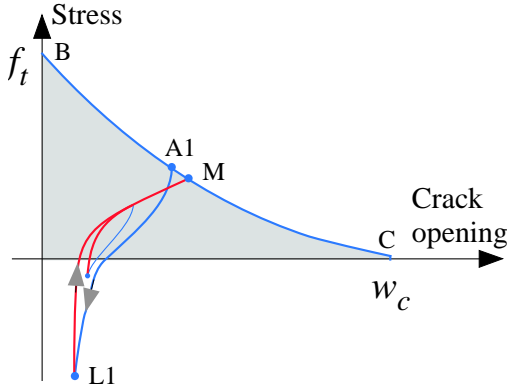


Figure 1. Cohesive stress-COD law.

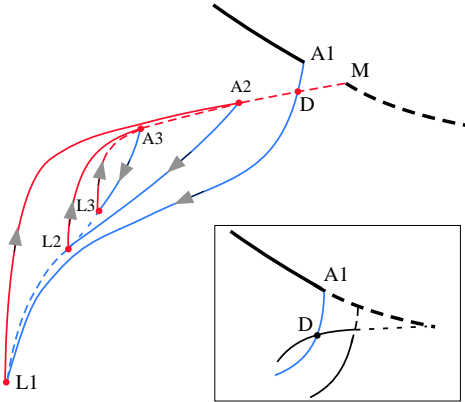


Figure 2. Hysteretic unloading and reloading loops according to the Continuous Function Model.

3 FINITE ELEMENT ANALYSIS

In this work, the continuum surrounding the process zone is taken to be *linear elastic*. All non-linear phenomena are assumed to occur in the *process zone*. When the fictitious crack tip advances by a pre-determined length, each point located along the crack trajectory is split into two points. The virtual mechanical entity, acting on these two points only, is called *cohesive element*: the local behaviour of such an element follows the rules described in the previous section. Each cohesive element interacts with the others only through the undamaged continuum, external to the process zone.

According to the finite element method, by taking the unknowns to be the n nodal displacement increments, $\Delta \mathbf{u}$, and assuming that compatibility and equilibrium conditions are satisfied at all points in the solid, we get the following system of n equations with $n + 1$ unknowns ($\Delta \mathbf{u}$, $\Delta \lambda$):

$$(\mathbf{K}_T + \mathbf{C}_T) \Delta \mathbf{u} = \Delta \lambda \mathbf{P} \quad (2)$$

where:

- \mathbf{K}_T : positive definite tangential stiffness matrix, containing contributions from linear elastic (undamaged) elements and possible contributions from cohesive elements having (σ, w) below the curve of Figure 1;
- \mathbf{C}_T : negative definite tangential stiffness matrix, containing contributions from cohesive elements with (σ, w) on the curve of Figure 1;
- \mathbf{P} : external load vector;
- $\Delta \lambda$: load multiplier increment. During the numerical analysis the stresses follow a piece-wise linear path. To obtain a good approximation of the non linear curves shown in Figure 1, $\Delta \lambda$ increments have to be small enough.

The above mentioned model was also successfully used in the numerical simulation of mixed-mode crack propagation, see Barpi & Valente (1998), Barpi & Valente (2000) as well as in crack propagation under constant load, see Barpi & Valente (2002) and Barpi & Valente (2003).

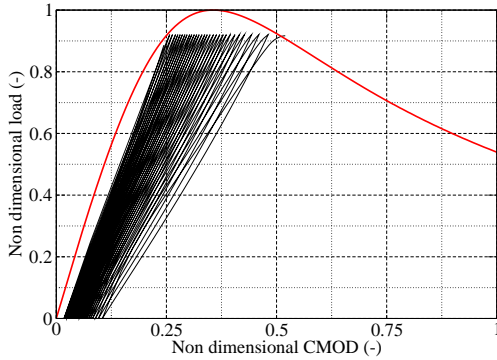


Figure 3. Non dimensional load vs. non dimensional CMOD ($\frac{P_{upper}}{P_{peak}} = 0.92$).

During the loading phase the stress paths of the cohesive elements are forced to stay on curve $B - A1$ of Figure 1, whereas during the cyclic loading phase they are forced to stay on the curves shown in Figure 2. The $A1 - L1 - A2$ stress path is called external loop and the $A2 - L2$ and $A3 - L3$ paths inner loops (Hordijk (1991)).

Fatigue rupture is reached when the smallest eigenvalue of the tangential stiffness matrix becomes negative: this condition means that the external load cannot reach the upper value P_{upper} any longer.

4 PRE-PEAK LOADING PROCEDURE

The loading procedure analysed is based on two phases. In the first, the external load grows from zero to the fatigue upper level (P_{upper}), a fraction of the peak load (P_{peak}). In the second, a cyclic loading condition is applied, from P_{upper} to P_{lower} and vice versa. In the case of three-point bending test, the global response in the nondimensional load-CMOD plane, is shown in Figure 3.

As the fictitious crack grows, the undamaged ligament reduces and structural compliance increases. The previously described fatigue rupture condition is achieved approximately when the global load path reaches the post-peak branch of the static curve. The results shown in Figure 3 has been obtained for the dimen-

Table 1. Geometrical and material parameters.

L/H	a_0/H	$\Delta H/H$	ν	H/l_{ch}	β	ε_u
8	1/3	1/160	0.1	1.193	0.055	$7.8 \cdot 10^{-5}$

sionless parameters presented in Table 1 where L/H represents the span to depth ratio, a_0/H the notch to depth ratio, $\Delta H/H$ the mesh size ratio, ν Poisson's ratio, $l_{ch} = \frac{E G_F}{\sigma_u^2}$ Hillerborg's characteristic length, H/l_{ch} the depth to characteristic length ratio, β the Huang-Li tension-softening constant and ε_u the ultimate tensile strain. The upper loading level is $\frac{P_{upper}}{P_{peak}} = 0.92$ and the lower loading level is $\frac{P_{lower}}{P_{peak}} = 0.0$.

5 VARIABLE AMPLITUDE FATIGUE LOADING INDUCED BY A SEISMIC EXCITATION

According to the original formulation (Hordijk (1991)) of the Continuous Function Model (CFM), at the beginning of the unloading step, point D in Figure 2 plays a crucial role:

- if the stress path is on the right of point D , point $A1$ moves in such a way that the related unloading path passes through the current point (dotted line in Figure 2). Therefore point $L1$ and M move too, the damage grows, and the current cycle can be locally considered as a *fatigue cycle*;
- if the stress path is on the left of point D , points $A1$, $L1$, M do not move, and an inner loop without damage occurs. The current cycle can be locally considered as a mere *loading cycle* and not as a fatigue cycle.

The above mentioned condition may vary from point to point along the FPZ. It is commonly accepted that under seismic excitation the frequency of the induced stresses in a concrete gravity dam ranges from 3 to 10 Hz. This load is far from being harmonic and is characterized by intermittent *spikes*. Therefore it is worthwhile analysing the behaviour of the above mentioned model during and after a load spike. At the peak value of a spike all stress paths in the FPZ are on the right of point D , or even on the right of point M . The next two steps

will be characterized by a large unloading step (second part of the spike cycle) followed by a small reloading step (first part of an ordinary cycle). As a consequence, all stress paths are on the left of point D and all ordinary cycles will be inner loops without damage until a new spike occurs. At this point it is possible to conclude that, according to the CFM, a spike decelerates crack growth at a subsequent lower load level. After a series of experimental tests, Slowik, Plizzari, & Saouma (1996) observed the opposite phenomenon: a spike accelerates crack growth at a subsequent lower load level. It is therefore possible to conclude that the use of the CFM in a finite element analysis entails results which are unrealistic and unconservative. This is a first reason to enhance the CFM by including the damage occurring during the so-called inner loops.

6 ENDURANCE LIMIT

In case of harmonic excitation, a load level exists below which no crack growth occurs. This load level is called *endurance limit*. For the dimensionless parameters listed in Table 1, Figure 4 shows the endurance limit as a function of size, obtained through the numerical simulation of three-point bending tests. After a series of experimental tests, Slowik, Plizzari, & Saouma (1996) observed lower values of the endurance limit. This is a second reason to enhance the CFM by including the damage occurring during the so-called inner loops.

7 A DAMAGE LAW FOR THE INNER LOOPS

Up to this point, the fatigue induced damage is related to the distance between points $A1$ and M in Figure 2. These points do not move during the so-called inner loops. In order to overcome the above mentioned problems, in this paper the CFM is enhanced by assuming a damage law for the inner loops too. More precisely, with reference to Figure 2, when the stress path is at point $L2$ or $L3$ (lower level of an inner loop), point M moves along the static envelope of 0.001 in a dimensionless plane. From a physical point of view, this fact represents a damage which occurs independently of the position of point $A2$. In other words it occurs during an inner loop as well as during an external loop. In order to

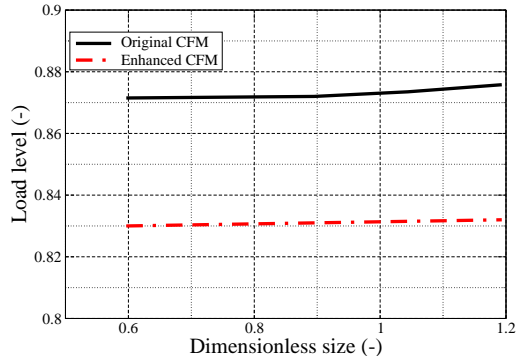


Figure 4. Size effects on endurance limit.

introduce an upper limit to this second type of damage, the damage process is stopped when point M moves to twice its original distance from point $A1$. This simple assumption modifies the numerical response in the direction indicated by the experimental evidence: the evolution of damage is no longer stopped by a loading spike. On the contrary, the ligament reduction induced by a spike accelerates crack growth after a subsequent lower load level. Considering a harmonic loading law, the endurance limit reduces from 0.875 to 0.832 in the case of a large sized structure ($H/l_{ch} = 1.193$), and from 0.872 to 0.830 in the case of a small sized one ($H/l_{ch} = 0.596$), as shown in Figure 4.

Finally, Figures 5 and 6 show the stress at the midspan section of the beam ($\frac{P_{upper}}{P_{peak}} = 0.92$) for $P = P_{lower}$ and $P = P_{upper}$, while Figure 7 show the stress paths (in the (σ, w) plane) relating to a cohesive element near the notch.

8 CONCLUSIONS

- In its original formulation, the Continuous Function Model (CFM) predicts that a higher preloading arrests the fatigue crack growth at a subsequent lower load level. This *unrealistic* and *unconservative* behaviour is due to the fact that the above mentioned model neglects the damage occurring during the so-called inner loops. In other words the CFM assumes that inner loops are mere loading loops and not fatigue

loops. This assumption causes an *incorrect prediction* of the sequence effect.

- For the same reason the CFM predicts an endurance limit which is *higher* than attested by experimental evidence.
- In order to obtain more realistic results, in the present paper, the CFM is enhanced, introducing a *damage mechanism* for the inner loops too.
- In the new model proposed, as well as in the original CFM, the endurance limit is seen to be an *almost constant* function of structural size.

9 ACKNOWLEDGMENTS

The financial support provided by the Italian Department of University and Scientific Research (MIUR) to the research project on “*Dam-reservoir-foundation systems: dynamic, diagnostic and safety analyses*” (grant number 200 2087915_006) is gratefully acknowledged.

REFERENCES

- Barpi, F. & S. Valente (1998). Size-effects induced bifurcation phenomena during multiple cohesive crack propagation. *International Journal of Solids and Structures* 35(16), 1851–1861.
- Barpi, F. & S. Valente (2000). Numerical simulation of prenotched gravity dam models. *Journal of Engineering Mechanics (ASCE)* 126(6), 611–619.
- Barpi, F. & S. Valente (2002). Fuzzy parameters analysis of time-dependent fracture of concrete dam models. *International Journal for Numerical and Analytical Methods in Geomechanics* 26, 1005–1027.
- Barpi, F. & S. Valente (2003). Creep and fracture in concrete: A fractional order rate approach. *Engineering Fracture Mechanics* 70, 611–623.
- Hillerborg, A., M. Modeer, & P. E. Petersson (1976). Analysis of crack formation and crack growth in concrete by means of fracture mechanics and finite elements. *Cement and Concrete Research* 6, 773–782.
- Hordijk, D. (1991). *Local approach to fatigue of concrete*. Ph. D. thesis, Delft University (The Netherlands).
- Huang, J. & V. Li (1989). A meso-mechanical model of the tensile behaviour of concrete. *Composites* 20, 370–378.
- Karihaloo, B. L. (1995). *Fracture Mechanics and Structural Concrete*. England: Longman Scientific and Technical.
- Slowik, V., G. Plizzari, & V. Saouma (1996). Fracture of concrete under variable amplitude fatigue loading. *American Concrete Institute Journal* 93(3), 272–283.

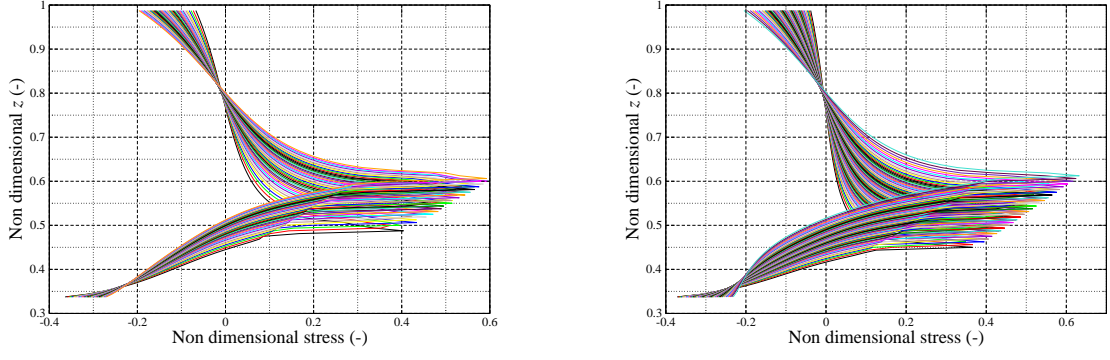


Figure 5. Non dimensional stress vs. z/H ($P = P_{lower}$) for $H/l_{ch} = 0.596$ (left) and 1.193 (right) at the midspan section of the beam.

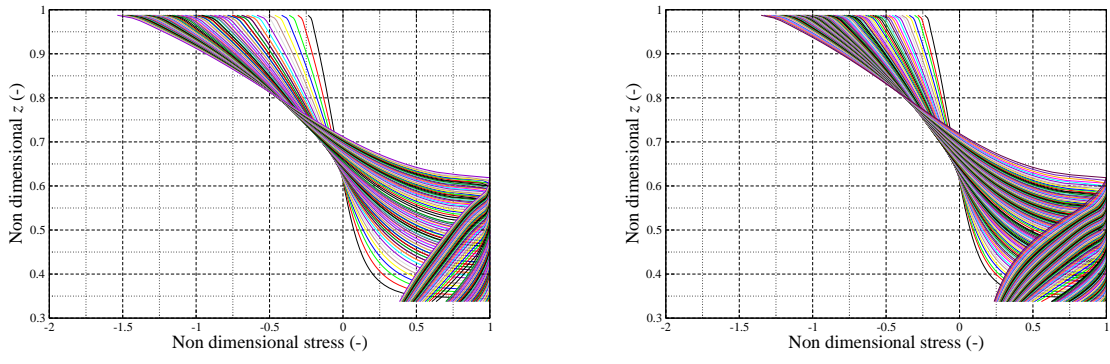


Figure 6. Non dimensional stress vs. z/H ($P = P_{upper}$) for $H/l_{ch} = 0.596$ (left) and 1.193 (right) at midspan section of the beam.

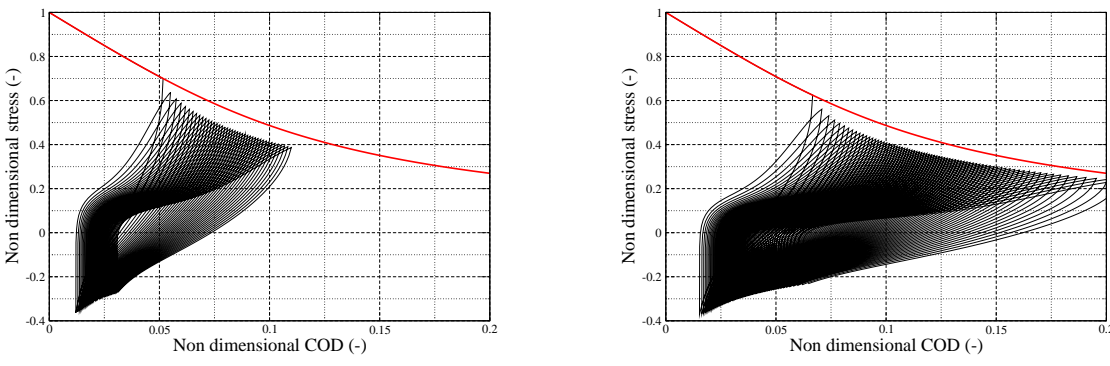


Figure 7. Stress paths at real crack tip ($\frac{P_{upper}}{P_{peak}} = 0.92$) for $H/l_{ch} = 0.596$ (left) and 1.193 (right).